The Zermelo-Voronoi Diagram: a Dynamic Partition Problem ⋆

Efstathios Bakolas [a] and Panagiotis Tsiotras [a]

[a] *School of Aerospace Engineering, Georgia Institute of Technology, Atlanta, GA 30332-0150, USA*

Abstract

We consider a Voronoi-like partition problem in the plane for a given finite set of generators. Each element in this partition is uniquely associated with a particular generator in the following sense: An agent that resides within a set of the partition at a given time will arrive at the generator associated with this set faster than any other agent that resides anywhere outside this set at the same instant of time. The agent's motion is affected by the presence of a temporally-varying drift, which is induced by local winds/currents. As a result, the minimum-time to a destination is not equivalent to the minimum-distance traveled. This simple fact has important ramifications over the partitioning problem. It is shown that this problem can be interpreted as a Dynamic Voronoi Diagram problem, where the generators are not fixed, but rather they are moving targets to be reached in minimum time. The problem is solved by first reducing it to a standard Voronoi Diagram by means of a time-varying coordinate transformation. We then extend the approach to solve the dual problem where the generators are the initial locations of a given set of agents distributed over the plane, such that each element in the partition consists of the terminal positions that can be reached by the corresponding agent faster than any other agent.

Key words: Autonomous agents, Voronoi Diagram, Zermelo-Voronoi Diagram, Dual Zermelo-Voronoi Diagram, computational methods, dynamic partition problems.

1 Introduction

The concept of the "Dirichlet-Voronoi Diagram," first introduced by Dirichlet in 1850 [12], and subsequently generalized by Voronoi in 1908 [24], has found a large spectrum of applications in different fields, including computer graphics, computer vision, computational geometry, robotics and, more recently, autonomous agents and mobile sensor networks [5,14,6,17,16,10,9]. Dirichlet-Voronoi Diagrams, known also as "Voronoi Diagrams/Tessellations" or "Thiessen Polygons," [1] describe a special partition of a topological space, which is equipped with a generalized distance function, where each element in the partition, known as the Dirichlet domain, is associated uniquely with an element from a given point-set, known as the set of *Voronoi generators*, based on the proximity relations between each point in the Dirichlet domain and its corresponding Voronoi generator. We shall refer to the partition problem of a subspace of the n-dimensional Euclidean space (with respect to the Euclidean distance) as the *standard Voronoi Diagram* problem, and as the *generalized Voronoi Diagram* problem otherwise. A detailed treatment of the Voronoi Diagram problem for a plethora of "distance" functions and topologies can be found in [6,20,2] and the references therein.

In many applications of autonomous agents, ranging from surveillance, optimal pursuit of multiple targets, environmental monitoring and vehicle routing problems, to mention a few, significant insight can be gleaned from data structures associated with Voronoi-like partitions. A typical application could be the following: given a number of landing sites, divide the area into distinct non-overlapping cells (one for each landing site) such that the corresponding site in the cell is the closest one (in terms of time) to land for any airplane/UAV flying over this cell in the presence of winds. A similar application that fits into the same framework is the task of subdividing the plane into "guard/safety zones," such that a guard/rescue vehicle residing within each particular zone can reach all points in its assigned zone faster

⋆ The material in this paper was partially presented at the 2010 American Control Conference, held at Baltimore, Maryland, USA, on June 30-July 2, 2010. Corresponding author P. Tsiotras. Tel. +(404) 894-9526. Fax (404) 894-2760.

Email addresses: ebakolas@gatech.edu (Efstathios Bakolas), tsiotras@gatech.edu (Panagiotis Tsiotras).

[1] Henceforth, we shall use the term "Voronoi Diagrams" which is the most commonly used terminology.

than any other guard/rescuer outside its zone. The common, underlying theme in these problems is the fact that they can be formulated as generalized minimum-distance problems where the relevant metric is the minimum intercept (or arrival) time.

The construction of generalized Voronoi diagrams with time as the distance metric (and several applications, especially those involving autonomous agent routing problems, such as those mentioned before, fall into this category) is, in general, a difficult task for two reasons. First, the distance metric is not symmetric and/or it may not be expressible in closed form. Second, such problems fall under the general case of partition problems for which the agents' dynamics must be taken into account [2]. The topology of the agent's configuration space may be non-Euclidean, for example, it may be a manifold embedded in a Euclidean space. In other words, these problems may not be reducible to generalized Voronoi Diagram problems, for which efficient construction schemes exist in the literature.

In this work we deal with the construction of Voronoi-like partitions that cannot be put under the umbrella of the available classes of generalized Voronoi Diagrams. In particular, we deal with Voronoi-like partitions in the plane for a given (finite) set of generators, such that each element in this partition is uniquely associated with a particular generator in the following sense: An agent that resides in a particular set of the partition at a given instant of time can arrive at the generator associated with this set faster than any other agent that may be located anywhere outside this set at the same instant of time. It is assumed that the agent's motion is affected by the presence of temporally-varying drift. Since the generalized distance of this Voronoi-like partition problem is the minimum time-to-go of the Zermelo's navigation problem [25], we shall henceforth refer to this partition of the configuration space as the Zermelo-Voronoi Diagram (ZVD).

The Zermelo-Voronoi Diagram problem therefore deals with a special partition of the Euclidean plane with respect to a generalized distance function, which is the minimum time of the Zermelo's navigation problem [25]. The characterization of this Voronoi-like partition will allow us to address questions dealing with the proximity relations between an agent (UAV/AUV) that travels in the presence of winds/currents and the set of Voronoi generators. For example the question of determining the generator from a given set which is the "closest," in terms of arrival time, to the agent at a particular instant of time, reduces to the problem of determining the set of the Zermelo-Voronoi partition that the agent resides in at the given instant of time (the latter question is known in the computational geometry parlance as the *point location* problem).

The main inspiration of our work is [23] where the ZVD problem has been treated for the case of constant drift. As shown in [23], the generalized Voronoi Diagram problem can be associated with a standard Voronoi Diagram by means of a coordinate transformation when the forward speed of the agent is greater than the magnitude of the drift. The approach presented in [23] is, however, of limited scope since it is based on constructive, geometric arguments that apply only to the constant drift case. In this work, we introduce a methodology that generalizes the results of [23] under a framework that may prove powerful for dealing with similar partition problems in the future. In particular, by adopting the interpretation of Zermelo's problem as a moving target problem [15], the ZVD problem is reduced to a standard Dynamic Voronoi Diagram problem, namely, a standard Voronoi Diagram where the Voronoi generators are not necessarily fixed, but rather they are moving targets [11,1,20]. This Dynamic Voronoi Diagram problem is dealt with by associating it with a standard Voronoi Diagram by means of a time-varying transformation in the case of a time-varying drift. Furthermore, we introduce the Dual Zermelo-Voronoi Diagram (DZVD) problem, which leads to a partition problem similar to the ZVD problem, with the difference that the generalized distance of the DZVD problem is the minimum time of the Zermelo navigation problem *from* a Voronoi generator *to* a point in the plane. Since the minimum time of the Zermelo navigation problem is not a symmetric function with respect to the initial and final configurations, the ZVD and the DZVD are not, in general, identical.

The case of non-stationary *spatially-varying* drift is more complex, and a (semi-)analytic treatment of that problem seems doubtful. To the authors' knowledge, the only available result in the literature that deals with spatially-varying (albeit stationary) drift are given in [18,19], where a purely computational/numerical solutions of the problem is presented. A more recent treatment of this problem is given in [3].

The rest of the paper is organized as follows. In Section 2 we formulate the Zermelo-Voronoi Diagram problem. In Section 3 the connection between the ZVD and the standard Dynamic Voronoi Diagram is demonstrated. In Sections 4 and 5 we present a scheme for the characterization of the ZVD and the DZVD based on a homeomorphism, which is applied to the standard Voronoi Diagram of the same set of Voronoi generators. Section 6 provides simulation results and, finally, Section 7 concludes the paper with a summary of remarks.

[2] A typical example is Voronoi-like partitions for a Dubins vehicle. See [21] for an initial treatment of this problem.

2 Problem Formulation

We will be dealing with the movement of autonomous mobile vehicles (agents) in the plane. It is assumed that the agent's motion is described by the following equation

$$\dot{\mathsf{x}} = u + w(t), \tag{1}$$

where $\mathsf{x} \triangleq (x, y)^\intercal \in \mathbb{R}^2$ is the position vector of the agent, $u \in \mathbb{R}^2$ is the control input and $w \triangleq (\mu, \nu)^\intercal \in \mathbb{R}^2$ is the drift, which is assumed to vary uniformly with time [3]. Note that w is to be interpreted as a time-varying velocity field induced by the winds/currents, which is assumed to be known a priori. In addition, it is assumed that $|w(t)| < 1$ for all $t \geq 0$, which implies, in turn, that the system (1) is completely controllable (see for example [7, p. 242]). Furthermore, the set of admissible control inputs is given by $\mathcal{U} \triangleq \{u \in \mathfrak{U}_{[0,T]} : u(t) \in U, \text{ for all } t \in [0,T],\ T > 0\}$, where $\mathfrak{U}_{[0,T]}$ is the set of all measurable functions on $[0,T]$, and $U = \{(u_1, u_2) \in \mathbb{R}^2 : u_1^2 + u_2^2 \leq 1\}$ (closed unit ball) is the corresponding input value set. The Zermelo's navigation problem (ZNP) can then be formulated as follows.

Problem 1 (ZNP) *Given the system described by equation* (1), *determine the control input* $u^* \in \mathcal{U}$ *such that*

i) The control u^* *minimizes the cost functional* $J(u) \triangleq T_\mathsf{f}$, *where* T_f *is the free final time.*
ii) The trajectory $\mathsf{x}^* : [0, T_\mathsf{f}] \mapsto \mathbb{R}^2$ *generated by the control* u^* *satisfies the boundary conditions*

$$\mathsf{x}^*(0) = \mathsf{x}_0, \quad \mathsf{x}^*(T_\mathsf{f}) = \mathsf{x}_\mathsf{f}. \tag{2}$$

The following proposition follows by virtue of Filippov's theorem on the existence of solutions for minimum-time problems [8, p. 311-317] and the complete controllability of the system (1) when $|w(t)| < 1$ for all $t \geq 0$ (see for example [7, p. 242]).

Proposition 2 *Let* x_0 *and* x_f *be two points in* $\mathbb{R}^2$. *If* $|w(t)| < 1$ *for all* $t \geq 0$, *then the system described by equation* (1) *admits a minimum-time path from* x_0 *to* x_f.

For more details the reader can refer to [8, p. 311-317].

It can be shown [7, p. 370-373] that the solution of Problem 1 when $w = w(t)$ is the control $u^*(\theta^*) = (\cos\theta^*, \sin\theta^*)$, where θ^* is a constant angle. It is worth noting that in the special case $w \equiv 0$, equation (1) becomes $\dot{\mathsf{x}} = u$, and subsequently the Zermelo's navigation problem is reduced to the shortest path problem in the plane.

Next, we formulate the Zermelo-Voronoi Diagram problem (ZVDP).

Problem 3 (ZVDP) *Given the system described by equation* (1), *a collection of goal destinations* $P \triangleq \{\mathsf{p}_i \in \mathbb{R}^2 : i \in \mathcal{I}\}$, *where* $\mathcal{I}$ *is a finite index set, and a transition cost*

$$c(\mathsf{x}_0, \mathsf{p}_i) \triangleq T_\mathsf{f}(\mathsf{x}_0, \mathsf{p}_i), \tag{3}$$

determine a partition $\mathfrak{V} = \{\mathfrak{V}_i : i \in \mathcal{I}\}$ *of* $\mathbb{R}^2$ *such that*

i) $\mathbb{R}^2 = \bigcup_{i \in \mathcal{I}} \mathfrak{V}_i$.
ii) $\overline{\mathfrak{V}_i} = \mathfrak{V}_i$, *for each* $i \in \mathcal{I}$.
iii) for each $\mathsf{x} \in \operatorname{int}(\mathfrak{V}_i)$, $c(\mathsf{x}, \mathsf{p}_i) < c(\mathsf{x}, \mathsf{p}_j)$ *for* $j \neq i$.

Henceforth, we shall refer to P, $\mathfrak{V}_i$, and $\mathfrak{V}$ as the set of *Voronoi generators* or *sites*, the *Dirichlet domain*, and the *Zermelo-Voronoi Diagram* of $\mathbb{R}^2$, respectively. In addition, two Dirichlet domains $\mathfrak{V}_i$ and $\mathfrak{V}_j$ are characterized as neighboring if they have a non-empty and non-trivial (i.e., single point) intersection.

Note that for the case $w \equiv 0$ Problem 3 reduces to the standard Voronoi Diagram problem. Next, we show that it is possible to associate the ZVDP with a standard Dynamic Voronoi Diagram, that is, a partitioning problem in the plane with respect to the Euclidean distance in the case of moving Voronoi generators, by means of a time-varying transformation.

Remark 1 In the problem formulation of the ZNP it is assumed that the drift $w(t)$ in equation (1), which is induced by the winds/currents, is known in advance over a sufficiently long (but finite) time horizon. This is possible if adequate weather forecast data over the area of interest are available. This is true, for example, in marine applications where the sea/river current (tides, etc) may be known beforehand.

3 The Zermelo-Voronoi Diagram Interpreted as a Dynamic Voronoi Diagram

The minimum time of the ZNP does not provide, in general, a generalized distance function that would allow one to reduce the ZVDP to a generalized Voronoi Diagram, for the construction of which efficient numerical techniques are available [6,20]. Therefore, one needs to adopt an alternative approach. Our strategy will be to associate Problem 3 with a standard Voronoi Diagram, which can be interpreted, in turn, as the solution of Problem 3 when $w \equiv 0$.

[3] In the original formulation of the Zermelo's navigation problem, the drift is assumed to be both spatially and temporally-varying. In this paper, we deal with the case of a temporally-varying drift only.

First, we observe that Problem 1 can be formulated alternatively as a moving target problem as follows.

Problem 4 (ZNMTP) *Given the system described by the equation*

$$\dot{\mathsf{X}} \triangleq \dot{\mathsf{x}} - w(t) = u(t), \quad \mathsf{X}(0) = \mathsf{x}_0 \tag{4}$$

determine the control input $u^* \in \mathcal{U}$ such that

i) The control u^* minimizes the cost functional $J(u) \triangleq T_{\mathsf{f}}$, where T_{f} is the free final time.
ii) The trajectory $\mathsf{X}^* : [0, T_{\mathsf{f}}] \mapsto \mathbb{R}^2$ generated by the control u^* satisfies the boundary conditions

$$\mathsf{X}^*(0) = \mathsf{x}_0, \qquad \mathsf{X}^*(T_{\mathsf{f}}) = \mathsf{x}_{\mathsf{f}} - \int_0^{T_{\mathsf{f}}} w(\tau)\,\mathrm{d}\tau. \tag{5}$$

It is clear that Problems 1 and 4 are equivalent, in the sense that a solution of Problem 1 is also a solution of Problem 4, and vice versa. Furthermore, an optimal trajectory X^* of Problem 4 is related to an optimal trajectory x^* of Problem 1 by means of the time-varying transformation

$$\mathsf{X}^*(t) = \mathsf{x}^*(t) - \int_0^t w(\tau)\mathrm{d}\tau. \tag{6}$$

The ZNMTP can be interpreted, in turn, as an optimal pursuit problem as follows: Given a pursuer and a moving target obeying the following kinematic equations

$$\dot{\mathsf{x}}_{\mathcal{P}} = \dot{\mathsf{X}} = u, \qquad \mathsf{x}_{\mathcal{P}}(0) = \mathsf{X}_0 = \mathsf{x}_0, \tag{7}$$
$$\dot{\mathsf{x}}_{\mathcal{T}} = -w(t), \qquad \mathsf{x}_{\mathcal{T}}(0) = \mathsf{x}_{\mathsf{f}}, \tag{8}$$

where $\mathsf{x}_{\mathcal{P}} = \mathsf{X}$, and $\mathsf{x}_{\mathcal{T}}$ are the coordinates of the pursuer and the moving target, respectively, find the optimal pursuit control law u such that the pursuer intercepts the moving target in minimum time T_{f}, that is,

$$\mathsf{x}_{\mathcal{P}}(T_{\mathsf{f}}) = \mathsf{X}(T_{\mathsf{f}}) = \mathsf{x}_{\mathcal{T}}(T_{\mathsf{f}}) = \mathsf{x}_{\mathsf{f}} - \int_0^{T_{\mathsf{f}}} w(\tau)\mathrm{d}\tau. \tag{9}$$

We have previously shown that the optimal control of Problem 1 is given by $u^* = (\cos\theta^*, \sin\theta^*)$ (x coordinates), where θ^* is a constant. Furthermore, equation (4) implies that the same control u^* is also the optimal control for the moving target Problem 3 (X coordinates). Figure 1 illustrates the optimal control strategy for the ZNMTP based on its interpretation as an optimal pursuit problem, where the pursuer and the moving target are denoted by a black and a green dot, respectively. Note that because the angle θ^* is necessarily constant, the pursuer is constrained to travel along a ray emanating from x_0 with constant unit speed (constant bearing angle pursuit strategy), whereas the target moves along the time-parameterized curve $\mathsf{x}_{\mathcal{T}} : [0, \infty) \mapsto \mathbb{R}^2$, where $\mathsf{x}_{\mathcal{T}}(t) = \mathsf{x}_{\mathsf{f}} - \int_0^t w(\tau)\,\mathrm{d}\tau$. From Proposition 2 it follows that there exists a time $T > 0$ such that $\mathsf{x}_{\mathcal{P}}(T) = \mathsf{X}(T) = \mathsf{x}_{\mathcal{T}}(T)$. The optimal value of θ^* corresponds to the least T, denoted as T_{f}, such that $\mathsf{x}_{\mathcal{P}}(T_{\mathsf{f}}) = \mathsf{X}(T_{\mathsf{f}}) = \mathsf{x}_{\mathcal{T}}(T_{\mathsf{f}})$. It is easy to show that the minimum time T_{f} is the least positive root of the following integral-algebraic equation

$$T = |\mathsf{x}_{\mathsf{f}} - \mathsf{x}_0 - \int_0^T w(\tau)\,\mathrm{d}\tau|, \tag{10}$$

whereas θ^* is given by

$$\theta^* = \mathrm{Arg}\left(\mathsf{x}_{\mathsf{f}} - \mathsf{x}_0 - \int_0^{T_{\mathsf{f}}} w(\tau)\,\mathrm{d}\tau\right). \tag{11}$$

It is worth mentioning here that the minimum time T_{f} is a directionally weighted (anisotropic) "distance" function, that is, the time to go from x_0 to x_{f}, and vice versa, not only depends on the Euclidean distance between these two points, but also on the direction of motion from x_0 and x_{f}. Therefore T_{f} is not a "true" distance function in the strict mathematical sense (the time to go from x_0 to x_{f} is, in general, different than the time to go from x_0 to x_{f} and therefore the symmetry axiom is not satisfied).

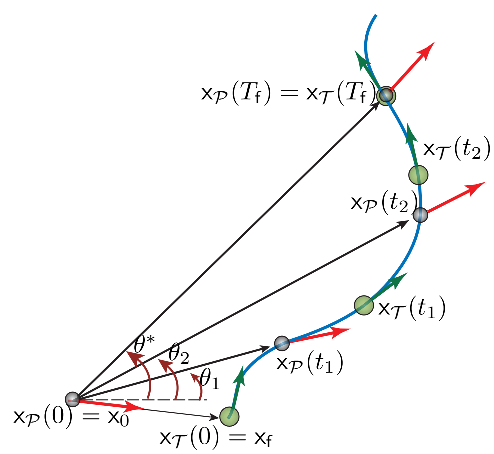

Fig. 1. Time-optimal control strategy for the ZNMTP interpreted as an optimal pursuit problem.

The idea of reducing the ZNP to a moving target problem in the Euclidean plane with no winds (ZNMTP), can also be applied to the ZVDP. In particular, the ZVDP can be formulated as a Dynamic Voronoi Diagram Problem (DVDP).

Problem 5 (DVDP) *Given the system described by equation (4), a collection of moving targets $P^d \triangleq \{\mathsf{P}_i : \mathsf{P}_i(t) = \mathsf{p}_i - \int_0^t w(\tau)\,\mathrm{d}\tau,\ i \in \mathcal{I}\}$, where $\mathcal{I}$ and p_i as in Problem 3, and a transition cost*

$$c^d(\mathsf{X}_0, \mathsf{P}_i) \triangleq |\mathsf{X}_0 - \mathsf{P}_i(T_{\mathsf{f}}(\mathsf{X}_0, \mathsf{p}_i))|, \tag{12}$$

determine a partition $V^d = \{V_i^d : i \in \mathcal{I}\}$ of $\mathbb{R}^2$ such that

i) $\mathbb{R}^2 = \bigcup_{i\in\mathcal{I}} V_i^d$.
ii) $\overline{V_i^d} = V_i^d$, *for each* $i \in \mathcal{I}$.
iii) For each $\mathsf{X} \in \mathrm{int}(V_i^d)$, *it follows that* $c^d(\mathsf{X}, \mathsf{P}_i) < c^d(\mathsf{x}, \mathsf{P}_j)$ *for* $j \neq i$.

Note that in the formulation of the DVDP the generalized distance function does not depend explicitly on time. The generalized distance function is the Euclidean distance between the initial configuration of the agent and the location of the moving target P_i at a specific instant of time, namely, $T_\mathsf{f}(\mathsf{x}_0, \mathsf{p}_i)$, that is, at the time when the pursuer, whose kinematics are described by equation (9), intercepts the moving target P_i (minimum intercept time). Figure 2 illustrates the interpretation of the ZVDP as a Dynamic Voronoi Diagram Problem. In particular, the target set, which is at time $t = 0$ the set of Voronoi generators $P = \{\mathsf{p}_i, i \in \mathcal{I}\}$ of the ZVDP, moves uniformly with time along the integral curves of the velocity field $-w$.

As it has been shown previously, the system (4) emanating from $\mathsf{X}(0) = \mathsf{X}_0$ reaches a point X_f in minimum time $T_\mathsf{f} = |\mathsf{X}_0 - \mathsf{X}_\mathsf{f}|$. Thus, by reversing time in (6), the system (1) starting from point x_0' at $t = 0$ reaches the point $\mathsf{x}_\mathsf{f} = \mathsf{X}_\mathsf{f}$ in minimum time $T_\mathsf{f} = |\mathsf{X}_0 - \mathsf{X}_\mathsf{f}|$, provided that

$$\mathsf{x}_0' = \mathsf{X}_0 - \int_0^{d(\mathsf{X}_0,\mathsf{X}_\mathsf{f})} w(\tau)\,\mathrm{d}\tau, \tag{13}$$

where $d(\mathsf{X}_0, \mathsf{X}_\mathsf{f}) \triangleq |\mathsf{X}_0 - \mathsf{X}_\mathsf{f}|$.

For each p, equation (13) induces a state transformation $f_\mathsf{p} : \mathbb{R}^2 \mapsto \mathbb{R}^2$ where

$$f_\mathsf{p}(\mathsf{X}) \triangleq \mathsf{X} - \int_0^{d(\mathsf{X},\mathsf{p})} w(\tau)\,\mathrm{d}\tau. \tag{14}$$

The following proposition will prove useful for the following discussion.

Proposition 6 *Let* $\mathsf{p} \in \mathbb{R}^2$ *be given. The state transformation in (14) defines a bijective mapping with nonsingular Jacobian for all* $\mathsf{X} \in \mathbb{R}^2$, *provided that* $|w(t)| < 1$ *for all* $t \geq 0$.

PROOF. First it is shown that f_p is an injective mapping. Let X_1 and X_2 be such that $f_\mathsf{p}(\mathsf{X}_1) = f_\mathsf{p}(\mathsf{X}_2)$, equivalently,

$$\mathsf{X}_2 - \mathsf{X}_1 = \int_{d(\mathsf{X}_2,\mathsf{p})}^{d(\mathsf{X}_1,\mathsf{p})} w(\tau)\,\mathrm{d}\tau. \tag{15}$$

Thus,

$$|\mathsf{X}_2 - \mathsf{X}_1| \leq \int_{d(\mathsf{X}_2,\mathsf{p})}^{d(\mathsf{X}_1,\mathsf{p})} |w(\tau)|\,\mathrm{d}\tau. \tag{16}$$

Since $|w(t)| < 1$ for all $t \geq 0$, it follows that

$$|\mathsf{X}_2 - \mathsf{X}_1| \leq |d(\mathsf{X}_1,\mathsf{p}) - d(\mathsf{X}_2,\mathsf{p})| \leq |\mathsf{X}_2 - \mathsf{X}_1|, \tag{17}$$

and thus $\mathsf{X}_2 = \mathsf{X}_1$. Furthermore, the Jacobian of f_p at X is equal to

$$Df_\mathsf{p}(\mathsf{X}) = I_2 - w(d(\mathsf{X},\mathsf{p}))(\mathsf{X} - \mathsf{p})^\mathsf{T}/d(\mathsf{X},\mathsf{p}). \tag{18}$$

It can be shown easily that the nonzero eigenvalue of the rank one matrix $w(d(\mathsf{X},\mathsf{p}))(\mathsf{X} - \mathsf{p})^\mathsf{T}/d(\mathsf{X},\mathsf{p})$ is given by

$$\lambda_2(\mathsf{X}) = w^\mathsf{T}(d(\mathsf{X},\mathsf{p}))(\mathsf{X} - \mathsf{p})/d(\mathsf{X},\mathsf{p}) \leq |w(d(\mathsf{X},\mathsf{p}))| < 1. \tag{19}$$

Thus $0 \notin \mathrm{spec}(Df_\mathsf{p}(\mathsf{X}))$ and the Jacobian $Df_\mathsf{p}(\mathsf{X})$ is nonsingular for all $\mathsf{X} \in \mathbb{R}^2$. Finally, because the Jacobian of F is nonsingular everywhere, it follows in light of the surjective mapping theorem [4, p. 378] that F is surjective.

The following two propositions follow readily from the previous discussion.

Proposition 7 *The coordinates of every element of the set* P *are invariant under the state transformation* (14), *that is,* $f_\mathsf{p}(\mathsf{p}) = \mathsf{p}$ *for all* $\mathsf{p} \in P$.

Proposition 8 *Let* $\mathsf{p} \in \mathbb{R}^2$ *be given. Then* $c(\mathsf{x}, \mathsf{p}) = |\mathsf{X} - \mathsf{p}|$ *provided that* $\mathsf{x} = f_\mathsf{p}(\mathsf{X})$.

In the next section, the interpretation of the ZNP as an optimal pursuit problem will allow us to associate the ZVD with the standard Voronoi diagram of the same set of generators by means of a homeomorphism which derives, in turn, from the state transformation (13).

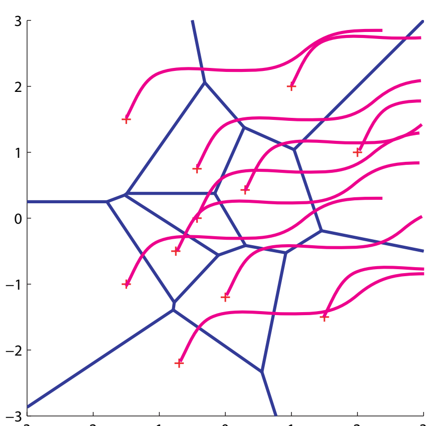

Fig. 2. The Zermelo-Voronoi Diagram can be interpreted as a Dynamic Voronoi Diagram.

Remark 2 Notice that although in this interpretation of the ZNP as a pursuer/moving target problem both the targets and (virtual) pursuers are moving, the Zermelo-Voronoi partition $\mathfrak{V}$ is independent of their motion after time $t = 0$. This is because it is assumed that each agent/pursuer follows the optimal min-time intercept strategy to each target. The final partition therefore already encodes the effect of the future motion of each agent and there is no need to re-compute the standard Voronoi partitions as the targets move along the integral curves of the (negative) velocity field.

4 Construction of the Zermelo-Voronoi Diagram

In this section, the steps required for the construction of the ZVD are demonstrated. In particular, it is shown that the state transformation (14) reduces the ZVD to a standard Voronoi Diagram for the case of two Voronoi generators. Subsequently, the previous result are generalized to the case of arbitrary finite sets of Voronoi generators.

Let us first consider two distinct points, p_1 and p_2, in the Euclidean plane. The bisector of p_1 and p_2 is the straight line $\chi(\mathsf{p}_1, \mathsf{p}_2)$ defined by

$$\begin{aligned}\chi(\mathsf{p}_1, \mathsf{p}_2) &\triangleq \left\{\mathsf{X} \in \mathbb{R}^2 : |\mathsf{X} - \mathsf{p}_1| = |\mathsf{X} - \mathsf{p}_2|\right\} \\ &= \left\{\mathsf{X} \in \mathbb{R}^2 : (\mathsf{p}_2 - \mathsf{p}_1)^{\mathsf{T}}\mathsf{X} = (|\mathsf{p}_2|^2 - |\mathsf{p}_1|^2)/2\right\}.\end{aligned}$$

Correspondingly, the bisector of p_1 and p_2 with respect to the cost (3) is the curve $\gamma(\mathsf{p}_1, \mathsf{p}_2)$ defined by

$$\gamma(\mathsf{p}_1, \mathsf{p}_2) \triangleq \{\mathsf{x} \in \mathbb{R}^2 : c(\mathsf{x}, \mathsf{p}_1) = c(\mathsf{x}, \mathsf{p}_2)\}. \qquad (20)$$

The bisector $\chi(\mathsf{p}_1, \mathsf{p}_2)$ divides $\mathbb{R}^2$ into two closed half-planes, namely $H_1(\mathsf{p}_1, \mathsf{p}_2) = \{\mathsf{X} \in \mathbb{R}^2 : |\mathsf{X} - \mathsf{p}_1| \leq |\mathsf{X} - \mathsf{p}_2|\}$ and $H_2(\mathsf{p}_1, \mathsf{p}_2) = \{\mathsf{X} \in \mathbb{R}^2 : |\mathsf{X} - \mathsf{p}_1| \geq |\mathsf{X} - \mathsf{p}_2|\}$.

The following proposition will allow us to associate the sets of points that are closer, in terms of the cost (3), to p_1 and p_2 with the half planes $H_1(\mathsf{p}_1, \mathsf{p}_2)$ and $H_2(\mathsf{p}_1, \mathsf{p}_2)$, respectively, by means of a homeomorphism.

Proposition 9 *Given $\mathsf{p}_1, \mathsf{p}_2 \in \mathbb{R}^2$, and a time-varying drift w, with $|w(t)| < 1$ for all $t \geq 0$, and let the function $F : \mathbb{R}^2 \mapsto \mathbb{R}^2$ be defined by*

$$F(\mathsf{X}) \triangleq \begin{cases} f_{\mathsf{p}_1}(\mathsf{X}), & \mathsf{X} \in H_1(\mathsf{p}_1, \mathsf{p}_2), \\ f_{\mathsf{p}_2}(\mathsf{X}), & \mathsf{X} \in H_2(\mathsf{p}_1, \mathsf{p}_2). \end{cases} \qquad (21)$$

Then the following statements are true.

i) The map F is continuous for all $\mathsf{X} \in \mathbb{R}^2$ and continuously differentiable for all $\mathsf{X} \notin \chi(\mathsf{p}_1, \mathsf{p}_2)$.

ii) The sets $F(H_1(\mathsf{p}_1, \mathsf{p}_2))$ and $F(H_2(\mathsf{p}_1, \mathsf{p}_2))$ are connected.

iii) The sets $F(H_1(\mathsf{p}_1, \mathsf{p}_2))$ and $F(H_2(\mathsf{p}_1, \mathsf{p}_2))$ are closed, and $\partial F(H_1(\mathsf{p}_1, \mathsf{p}_2)) = \partial F(H_2(\mathsf{p}_1, \mathsf{p}_2)) = F(\chi(\mathsf{p}_1, \mathsf{p}_2))$.

iv) $\mathrm{int}(F(H_1(\mathsf{p}_1, \mathsf{p}_2))) \cap \mathrm{int}(F(H_2(\mathsf{p}_1, \mathsf{p}_2))) = \varnothing$ and $F(H_1(\mathsf{p}_1, \mathsf{p}_2)) \cap F(H_2(\mathsf{p}_1, \mathsf{p}_2)) = F(\chi(\mathsf{p}_1, \mathsf{p}_2))$.

v) The map F is a homeomorphism.

vi) $\mathsf{p}_1 \in \mathrm{int}(F(H_1(\mathsf{p}_1, \mathsf{p}_2)))$ and $\mathsf{p}_2 \in \mathrm{int}(F(H_2(\mathsf{p}_1, \mathsf{p}_2)))$.

vii) For all $\mathsf{x} \in \mathrm{int}(F(H_1(\mathsf{p}_1, \mathsf{p}_2)))$, $c(\mathsf{x}, \mathsf{p}_1) < c(\mathsf{x}, \mathsf{p}_2)$. Similarly, for all $\mathsf{x} \in \mathrm{int}(F(H_2(\mathsf{p}_1, \mathsf{p}_2)))$, $c(\mathsf{x}, \mathsf{p}_2) < c(\mathsf{x}, \mathsf{p}_1)$.

viii) The bisector of p_1 and p_2 with respect to the cost c satisfies

$$\gamma(\mathsf{p}_1, \mathsf{p}_2) = \{\mathsf{x} \in \mathbb{R}^2 : \mathsf{x} = F(\mathsf{X}),\ \mathsf{X} \in \chi(\mathsf{p}_1, \mathsf{p}_2)\}.$$

PROOF.

i) First, we show that F is well defined for $\mathsf{X} \in H_1(\mathsf{p}_1, \mathsf{p}_2) \cap H_2(\mathsf{p}_1, \mathsf{p}_2) = \chi(\mathsf{p}_1, \mathsf{p}_2)$. In particular, for $\mathsf{X} \in \chi(\mathsf{p}_1, \mathsf{p}_2)$, we have that $d(\mathsf{X}, \mathsf{p}_1) = d(\mathsf{X}, \mathsf{p}_2)$, which implies that $f_{\mathsf{p}_1}(\mathsf{X}) = f_{\mathsf{p}_2}(\mathsf{X})$. The continuity of F follows readily. Furthermore, the Jacobian of F is well defined and invertible (see Proposition 6) for all $\mathsf{X} \in \mathbb{R}^2 \backslash \chi(\mathsf{p}_1, \mathsf{p}_2)$, and it is given by (18) for X in $H_1(\mathsf{p}_1, \mathsf{p}_2)$ and $H_2(\mathsf{p}_1, \mathsf{p}_2)$, respectively.

ii) It follows immediately from the continuity of F.

iii) First, notice that the restriction of F on $H_1(\mathsf{p}_1, \mathsf{p}_2)$, is f_{p_1} which is an injective, continuously differentiable map with non-singular Jacobian (Proposition 6). It follows that f_{p_1} is a diffeomorphism from $H_1(\mathsf{p}_1, \mathsf{p}_2)$ to $F(H_1(\mathsf{p}_1, \mathsf{p}_2)) = f_{\mathsf{p}_1}(H_1(\mathsf{p}_1, \mathsf{p}_2))$ and therefore $F(H_1(\mathsf{p}_1, \mathsf{p}_2))$ is closed since $H_1(\mathsf{p}_1, \mathsf{p}_2))$ is closed. Furthermore, $\partial F(H_1(\mathsf{p}_1, \mathsf{p}_2)) = F(\partial H_1(\mathsf{p}_1, \mathsf{p}_2)) = F(\chi(\mathsf{p}_1, \mathsf{p}_2))$. The proof for $F(H_2(\mathsf{p}_1, \mathsf{p}_2))$ is similar.

iv) Assume, on the contrary, that there exists $\mathsf{y} \in \mathrm{int}(F(H_1(\mathsf{p}_1, \mathsf{p}_2))) \cap \mathrm{int}(F(H_2(\mathsf{p}_1, \mathsf{p}_2)))$. It follows from iii) that there are points $\mathsf{X}_1 \in \mathrm{int}(H_1(\mathsf{p}_1, \mathsf{p}_2))$ and $\mathsf{X}_2 \in \mathrm{int}(H_2(\mathsf{p}_1, \mathsf{p}_2))$ with $F(\mathsf{X}_1) = F(\mathsf{X}_2) = \mathsf{y}$. Thus $c(F(\mathsf{X}_1), \mathsf{p}_1) = c(F(\mathsf{X}_2), \mathsf{p}_1)$ and $c(F(\mathsf{X}_1), \mathsf{p}_2) = c(F(\mathsf{X}_2), \mathsf{p}_2)$, which imply, using Proposition 8, that $|\mathsf{X}_1 - \mathsf{p}_1| = |\mathsf{X}_2 - \mathsf{p}_1| = \delta_1$ and $|\mathsf{X}_1 - \mathsf{p}_2| = |\mathsf{X}_2 - \mathsf{p}_2| = \delta_2$ respectively, for some positive constants δ_1 and δ_2. Thus X_1 and X_2 lie necessarily at the intersection of two circles centered at p_i with radii δ_i, $i \in \{1, 2\}$, respectively. This intersection is nonempty if one of the following conditions hold true: a) $\delta_1 < \delta_2$ with $|\mathsf{p}_1 - \mathsf{p}_2| \leq \delta_1 + \delta_2$, which implies that both X_1 and X_2 are in $H_1(\mathsf{p}_1, \mathsf{p}_2)$, b) $\delta_1 > \delta_2$ with $|\mathsf{p}_1 - \mathsf{p}_2| \leq \delta_1 + \delta_2$, which implies that both X_1 and X_2 are in $H_2(\mathsf{p}_1, \mathsf{p}_2)$ and finally, c) $\delta_1 = \delta_2$ with $|\mathsf{p}_1 - \mathsf{p}_2| \leq \delta_1 + \delta_2$, which implies that both X_1 and X_2 are in $\chi(\mathsf{p}_1, \mathsf{p}_2)$. All previous cases contradict the assumption that $\mathsf{X}_1 \in \mathrm{int}(H_1(\mathsf{p}_1, \mathsf{p}_2))$

and $X_2 \in \text{int}(H_2(p_1, p_2))$. The second part of the statement follows readily.

v) First, we show that F is injective. First, notice that, by definition, F is injective on $H_1(p_1, p_2)$ and $H_2(p_1, p_2)$. Let now $X_1 \in \text{int}(H_1(p_1, p_2))$ and $X_2 \in \text{int}(H_2(p_1, p_2))$ and assume, on the contrary, that $F(X_1) = F(X_2)$. But $F(X_1) \in F(\text{int}(H_1(p_1, p_2))) \subseteq \text{int}(F(H_1(p_1, p_2)))$ since the restriction of F on $H_1(p_1, p_2)$ is an open map. Similarly, $F(X_2) \in F(\text{int}(H_2(p_1, p_2))) \subseteq \text{int}(F(H_2(p_1, p_2)))$. Hence $F(X_1) = F(X_2)$ implies that $\text{int}(F(H_1(p_1, p_2))) \cap \text{int}(F(H_2(p_1, p_2))) \neq \varnothing$, which contradicts iv). Since F is injective it follows readily that its inverse F^{-1} exists and it is defined by

$$F^{-1}(x) \triangleq \begin{cases} f_{p_1}^{-1}(x), & x \in F(H_1(p_1, p_2)), \\ f_{p_2}^{-1}(x), & x \in F(H_2(p_1, p_2)), \end{cases}$$

with $f_{p_1}^{-1}$ and $f_{p_2}^{-1}$ continuous on $H_1(p_1, p_2)$ and $H_2(p_1, p_2)$, respectively. Next we show that F^{-1} is a continuous function for all $x \in \mathbb{R}^2$. It suffices to show that F^{-1} is well defined for $x \in F(H_1(p_1, p_2)) \cap F(H_2(p_1, p_2)) = F(\chi(p_1, p_2))$. To this end, notice that the statement $x \in F(\chi(p_1, p_2))$ implies that there exists $X \in \chi(p_1, p_2)$ such that $x = F(X)$. But $X \in \chi(p_1, p_2)$ implies that $|X - p_1| = |X - p_2|$ and hence $x = f_{p_1}(X) = f_{p_2}(X)$. It follows that $f_{p_1}^{-1}(x) = f_{p_2}^{-1}(x)$ for all $x \in F(\chi(p_1, p_2))$.

vi) Since $p_1 \in \text{int}(H_1(p_1, p_2))$ $[p_2 \in \text{int}(H_2(p_1, p_2))]$ and the restriction of F on $\text{int}(H_1(p_1, p_2))$ $[\text{int}(H_2(p_1, p_2))]$ yields an open map, it follows that $p_1 = F(p_1) \in F(\text{int}(H_1(p_1, p_2))) \subset \text{int}(F(H_1(p_1, p_2)))$ $[p_2 \in \text{int}(F(H_2(p_1, p_2)))]$.

vii) Let us assume, on the contrary, that there exists $x \in \text{int}(F(H_1(p_1, p_2)))$ such that $c(x, p_1) \geq c(x, p_2)$. Let $X \in H_1(p_1, p_2)$ such $x = F(X)$. Note that iii) implies that $X \in \text{int}(H_1(p_1, p_2))$. It follows from Proposition 8 that $|X - p_1| \geq |X - p_2|$, contradicting the fact that $X \in \text{int}(H_1(p_1, p_2))$.

viii) The proof follows from iii), vii) and Proposition 8.

Figure 3 illustrates how the half-planes $H_1(p_1, p_2)$ and $H_2(p_1, p_2)$ and the bisector curve $\chi(p_1, p_2)$ (Fig. 3(a)) are transformed under the mapping F (Fig. 3(b)). Note that every point in $\chi(p_1, p_2)$ is equidistant, with respect to the Euclidean distance, to p_1 and p_2, and the same is true for the curve $\gamma(p_1, p_2)$, which is the image of $\chi(p_1, p_2)$ under F, with respect, however, to the generalized distance function (3). Furthermore, if $A \in \chi(p_1, p_2)$ with $|p_1 - \overrightarrow{OA}| = |p_2 - \overrightarrow{OA}| = \delta$, then it also holds that $T_f(C, p_1) = T_f(C, p_2) = \delta$, where the point C lies on the curve $\gamma(p_1, p_2)$ and satisfies $\overrightarrow{OC} = F(\overrightarrow{OA})$.

Proposition 9 deals with the construction of the ZVD in the special case $P = \{p_1, p_2\}$. In particular, it implies that $\mathfrak{V} = \{\mathfrak{V}_1, \mathfrak{V}_2\}$, where $\mathfrak{V}_1 = F(H_1(p_1, p_2))$ and $\mathfrak{V}_2 = F(H_2(p_1, p_2))$. Furthermore, the standard Voronoi Diagram of $P = \{p_1, p_2\}$ is given by $V = \{V_1, V_2\}$, where $V_1 = H_1(p_1, p_2)$ and $V_2 = H_2(p_1, p_2)$. Therefore, $\mathfrak{V} = \{F(V_1), F(V_2)\}$. We are now ready to state the main theorem of this paper.

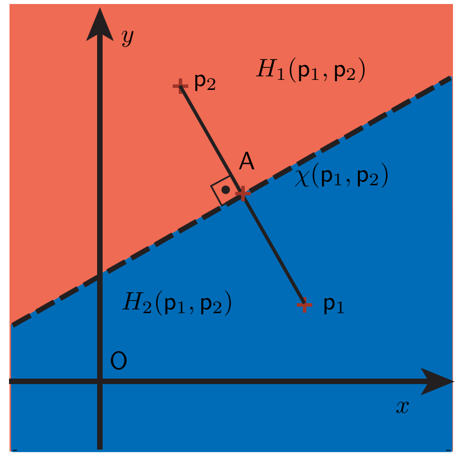

(a) The bisector χ and the two half planes $H_1(p_1, p_2)$ and $H_2(p_1, p_2)$.

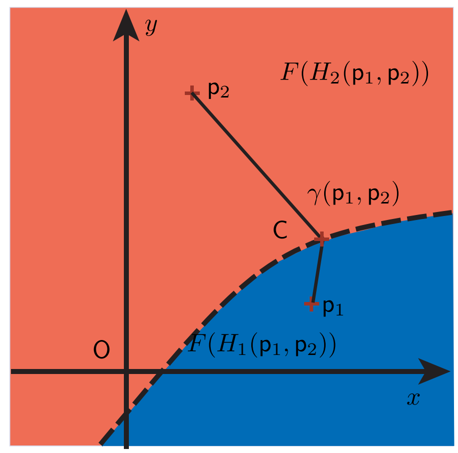

(b) The images of χ, $H_1(p_1, p_2)$ and $H_2(p_1, p_2)$ under the mapping F.

Fig. 3. The image of the bisector $\chi(p_1, p_2)$ under the mapping F, denoted as $\gamma(p_1, p_2)$, is the bisector of p_1 and p_2 with respect to the generalized distance function of Problem 2.

Theorem 10 *Let $V \triangleq \{V_i, i \in \mathcal{I}\}$ be the standard Voronoi partition for the set of Voronoi generators $P \triangleq \{p_i, i \in \mathcal{I}\}$. Assume that $|w(t)| < 1$, for all $t \geq 0$ and let the function $F : \mathbb{R}^2 \mapsto \mathbb{R}^2$ be defined by*

$$F(X) = f_{p_i}(X), \qquad X \in V_i, \ i \in \mathcal{I}, \tag{22}$$

where

$$f_{p_i}(X) = X - \int_0^{d(X, p_i)} w(\tau)\, d\tau, \quad i \in \mathcal{I}. \tag{23}$$

The solution of the ZVDP is the partition defined by the image of V under the mapping F, that is,

$$\mathfrak{V} \triangleq \{\mathfrak{V}_i : \ i \in \mathcal{I}\} = F(V) \triangleq \{f_{\mathsf{p}_i}(V_i) : \ \ i \in \mathcal{I}\}, \quad (24)$$

or equivalently, $\mathfrak{V}_i = f_{\mathsf{p}_i}(V_i)$ for all $i \in \mathcal{I}$.

PROOF. The Dirichlet domain V_i of the standard Voronoi partition V is determined by [14]

$$V_i = \bigcap_{j \neq i} H_i(\mathsf{p}_i, \mathsf{p}_j). \quad (25)$$

Thus

$$F(V_i) = F(\bigcap_{j \neq i} H_i(\mathsf{p}_i, \mathsf{p}_j)), \quad (26)$$

which implies, by virtue of F being injective (Proposition 9(v)), that $F(V_i) = \bigcap_{j \neq i} F(H_i(\mathsf{p}_i, \mathsf{p}_j))$. The proof can be carried out similarly to Proposition 9 using induction.

Corollary 11 *Let $\mathfrak{V} \triangleq \{F(V_i) : \ i \in \mathcal{I}\}$ be the Voronoi partition for the set of Voronoi generators $P \triangleq \{\mathsf{p}_i, i \in \mathcal{I}\}$ of Problem 3. Then*

i) The sets $F(V_i)$ are closed and connected.
ii) $\mathsf{p}_i \in \operatorname{int}(F(V_i))$.
iii) if $\mathsf{p}_i \in \partial\operatorname{co}(P)$, where $\operatorname{co}(P)$ denotes the convex hull of the set P, then $F(V_i)$ is an unbounded set, and it is a compact set otherwise.

PROOF. The proofs of (i) and (ii) follow similarly as the proofs of (i), (ii) and (vi) of Proposition 9. To prove (iii), first note that a Dirichlet domain V_i of the standard Voronoi Diagram of P is an unbounded set if and only if $\mathsf{p}_i \in \partial\operatorname{co}(P)$ [14] and it is a compact set otherwise. Thus, by virtue of (v) of Proposition 9 the Dirichlet domain $F(V_i) = \mathfrak{V}_i$ that corresponds to $\mathsf{p}_i \in \partial\operatorname{co}(P)$ is an unbounded set. Finally, if $\mathsf{p}_i \notin \partial\operatorname{co}(P)$ then the Dirichlet domain V_i and its image under the continuous mapping F are both compact sets.

5 The Dual Zermelo-Voronoi Diagram

So far, we have presented a methodology for constructing the generalized Voronoi Diagram with respect to the minimum time from a point in plane to the set of generators (obtained from the solution of Zermelo's navigation problem). In many autonomous agent applications, however, it may be more appropriate to consider the Voronoi generators to be the agents' locations at a particular instant of time rather than being the goal destinations. For instance, consider the following scenario: Given a group of agents/guards distributed over a certain area, divide this area into guard/patrol zones (one for each agent) such that each point in a zone can be reached/intercepted by the corresponding agent faster than any other agent. Such a decomposition essentially provides a "first response" partition of the area for which the agents are responsible.

In this context, given the positions of a finite set of agents at time $t = 0$, we want to characterize for every $i \in \mathcal{I}$, where $\mathcal{I}$ denotes the index set of the set of agents, the collections of all positions, denoted as $\tilde{\mathfrak{V}}_i$, that can be reached by the agent i faster than any other agent j, with $j \neq i$. We call the problem of characterizing the partition $\tilde{\mathfrak{V}} \triangleq \{\tilde{\mathfrak{V}}_i : \ \ i \in \mathcal{I}\}$ the Dual Zermelo-Voronoi Diagram Problem (DZVDP).

Note that, as already mentioned, the minimum time of the ZNP is, in general, non-symmetric, that is, the minimum time to drive the system (1) from a point A to B, and vice versa, are not necessarily equal. Therefore the solutions of the DZVDP and the ZVDP are not expected to be the same, in general.

The DZVDP can be formulated similarly to the ZVDP. In particular, the distance function for the DZVDP is defined by

$$\tilde{c}(\mathsf{p}_i, \mathsf{x}_\mathsf{f}) \triangleq T_\mathsf{f}(\mathsf{p}_i, \mathsf{x}_\mathsf{f}), \quad (27)$$

that is, the minimum time for the Zermelo navigation problem from a Voronoi generator p_i to the agent's terminal configuration x_f. The generalized distance function for the DZVDP can be reduced to the distance function for the ZVDP by reversing the order of the function arguments. The construction of the DZVDP is thus similar to the solution of the ZVDP.

Corollary 12 *Let $V \triangleq \{V_i : \ \ i \in \mathcal{I}\}$ be the standard Voronoi partition for the set of Voronoi generators $P \triangleq \{\mathsf{p}_i : \ i \in \mathcal{I}\}$. Assume that $|w(t)| < 1$ for all $t \geq 0$ and let the function $\tilde{F} : \mathbb{R}^2 \mapsto \mathbb{R}^2$ be defined by*

$$\tilde{F}(\mathsf{X}) \triangleq \tilde{f}_{\mathsf{p}_i}(\mathsf{X}), \qquad \mathsf{X} \in V_i, \quad i \in \mathcal{I}, \quad (28)$$

where

$$\tilde{f}_{\mathsf{p}_i}(\mathsf{X}) \triangleq \mathsf{X} + \int_0^{d(\mathsf{X}, \mathsf{p}_i)} w(\tau)\, \mathrm{d}\tau, \quad i \in \mathcal{I}. \quad (29)$$

Then the solution of the DZVDP is the partition be defined by the image of the set V under the mapping $\tilde{F}$, that is,

$$\tilde{\mathfrak{V}} \triangleq \{\tilde{\mathfrak{V}}_i : \ \ i \in \mathcal{I}\} = \tilde{F}(V) = \{\tilde{f}_{\mathsf{p}_i}(V_i) : \ \ i \in \mathcal{I}\}, \quad (30)$$

or equivalently, $\tilde{\mathfrak{V}}_i \triangleq \tilde{f}_{\mathsf{p}_i}(V_i)$, for all $i \in \mathcal{I}$.

Note that the transformation (29) of the DZVDP differs from the transformation (23) of the ZVDP by a sign change.

6 Simulation Results

In this section numerical simulations to demonstrate the previous developments are provided. Let us consider the wind velocity field defined by

$$w(t) = \begin{cases} \bar{w} + \rho t, & 0 \le t \le \bar{t}, \\ \bar{w} + \rho \bar{t}, & t > \bar{t}, \end{cases} \tag{31}$$

where $\bar{w} = (\mu, \nu)^\mathsf{T} \in \mathbb{R}^2$ with $|\bar{w}| < 1$, $\rho \in \mathbb{R}^2$ constants, and $\bar{t} < (1 - |\bar{w}|)/|\rho|$.

We first construct the Zermelo-Voronoi Diagram by gridding the entire space and propagating the isocost fronts of the respective min-time problems emanating from each generator and we compare the results with the proposed approach of this paper in terms of computational efficiency. In particular, given a set of Voronoi generators $P \triangleq \{\mathsf{p}_i : \ i \in \mathcal{I}\}$, the minimum cost-to-go from x to some $\mathsf{p}_i \in P$ is defined as the function

$$K_{\mathsf{p}_i}(\mathsf{x}) \triangleq c(\mathsf{x}, \mathsf{p}_i). \tag{32}$$

Note that for the particular wind field in (31), it follows readily that $c(\mathsf{x}, \mathsf{p}_i)$ is the smallest positive root of either the polynomial equation

$$\frac{|\rho|^2}{4} T_\mathsf{f}^4 + \bar{w}^\mathsf{T} \rho T_\mathsf{f}^3 + (|\bar{w}|^2 - 1 - (\mathsf{p}_i - \mathsf{x})^\mathsf{T} \rho) T_\mathsf{f}^2 - 2(\mathsf{p}_i - \mathsf{x})^\mathsf{T} \bar{w} T_\mathsf{f} + |\mathsf{p}_i - \mathsf{x}|^2 = 0, \tag{33}$$

if $T_\mathsf{f} < \bar{t}$, or the quadratic equation

$$(|\bar{w} + \rho \bar{t}| - 1) T_\mathsf{f}^2 - (2(\mathsf{p}_i - \mathsf{x}) + \bar{t}^2 \rho)^\mathsf{T} (\bar{w} + \rho \bar{t}) T_\mathsf{f} + |\mathsf{p}_i - \mathsf{x}|^2 + \bar{t}^2 (\mathsf{p}_i - \mathsf{x})^\mathsf{T} \rho + \bar{t}^2 |\rho|^2 / 4 = 0, \tag{34}$$

if $T_\mathsf{f} \ge \bar{t}$. Furthermore, the minimum cost-to-go to the set P is defined as the function

$$K_P(\mathsf{x}) = \min_{\mathsf{p}_i \in P} c(\mathsf{x}, \mathsf{p}_i). \tag{35}$$

Each Dirichlet domain of the ZVD can be determined by projecting the intersection of the surfaces K_P and K_{p_i} onto $\mathbb{R}^2$. Figure 4 illustrates a fine approximation of the ZVD, which is constructed by the previous exhaustive numerical method for $\bar{w} = (-0.3, 0.2)$, $\rho = (0.05, -0.1)$, and a set of eleven Voronoi generators.

An alternative approach, instead of solving directly the polynomial equations in (33)-(34) for each node of a fine grid that discretizes the space, is to expand the iso-cost fronts of each K_p by means of a fast marching algorithm. The fast marching implementation will give an approximation of the ZVD with time complexity $O(NM^2 \log M)$, where N is the number of elements of P, and M^2 is the number of nodes of a grid that discretizes $\mathbb{R}^2$ [22,18]. Note that the boundaries of each Dirichlet domain of the ZVD are not line segments, in general, and thus for their specification a fine grid is required, that is, the size of the grid should be at least $O(N^\eta)$, where $\eta > 2$.

Next, the approach introduced in this paper is applied. In particular, the standard Voronoi Diagram of the set P is first constructed, and subsequently, the Zermelo-Voronoi Diagram is obtained with the application of Theorem 1. Note that the construction of the standard Voronoi Diagram requires $O(N \log N)$ time, where N is the number of elements of P, by using, for example, Fortune's algorithm [13]. The mapping of the standard Voronoi Diagram, which consists of $O(N)$ edges, to the ZVD requires $O(N)$ time, giving a total time complexity for the construction of the ZVD which is of order $O(N \log N)$. Note, additionally, that the approach of this paper is completely grid-free, and it does not also require the solution of a PDE by contrast to the fast marching approach. These remarks elucidate the significance of the results presented in Section 4 from a computational perspective. Figure 5 illustrates the ZVD obtained after the application of the state-transformation to the standard Voronoi Diagram.

Figure 6 illustrates the ZVD and the DZVD partitions for the wind velocity fields $w_1(t) = (0.5 + 0.1\sin(t/\pi), -0.35 - 0.1\cos(t/\pi))$ (Fig. 6(a)) and $w_2(t) = (0.15, 0.65 - 0.2\exp(-t/\pi))$ (Fig. 6(b)). It is interesting to note that, as the drift becomes stronger, the Voronoi generators move closer to the boundaries of their corresponding Dirichlet domains, following a pattern that is more complex than the one observed in [23]. This is due to the temporal variation of the drift. In all cases, however, the generators remain interior to their corresponding domains, in light of Proposition 9 (vi), provided that $|w(t)| < 1$ for all $t \ge 0$.

7 Conclusion

In this work we have addressed the problem of characterizing the Zermelo-Voronoi Diagram, which is a Voronoi-like partition for a given set of generators and a generalized distance function. In particular, the "distance" function is the minimum time required for an agent to reach the set of generators in the presence of time-varying drift. It is demonstrated that the Zermelo-Voronoi Diagram problem is essentially a dynamic partition problem, where the Voronoi generators are moving targets that travel along the integral curves of a velocity field, which is the opposite of the one induced

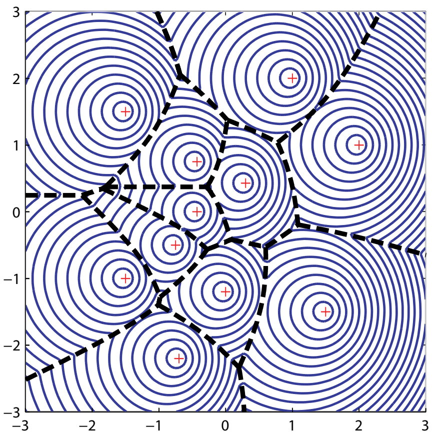

Fig. 4. The ZVD and the minimum cost-to-go interpretation. Computation using exhaustive numerical calculations of the min-time wavefronts.

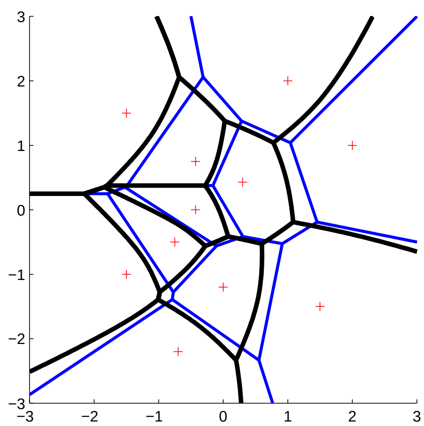

Fig. 5. The ZVD (black) and its corresponding standard Voronoi Diagram (blue). Computation using the computational scheme proposed in this paper.

by the time-varying drift. Subsequently, the Zermelo-Voronoi Diagram is associated with a standard Voronoi Diagram by means of a homeomorphism. By switching the roles of moving agent/target site we are led to the construction of the Dual Zermelo-Voronoi Diagram, which encodes all points in the plane that can be reached/intercepted by an agent initially located at the corresponding generator of a given Zermelo-Voronoi cell faster than any other agent outside this cell. Applications of the theory range from optimal routing and target allocation for small UAVs, distributed surveillance and minimum-time intercept of multiple targets over a given area, and minimum-time landing site selection for a group of airplanes, among others.

Acknowledgement: This work has been supported in part by NASA (award no. NNX08AB94A). The first author also acknowledges support from the A. Onassis Public Benefit Foundation. The authors would also like to thank the anonymous reviewers for their constructive comments and suggestions.

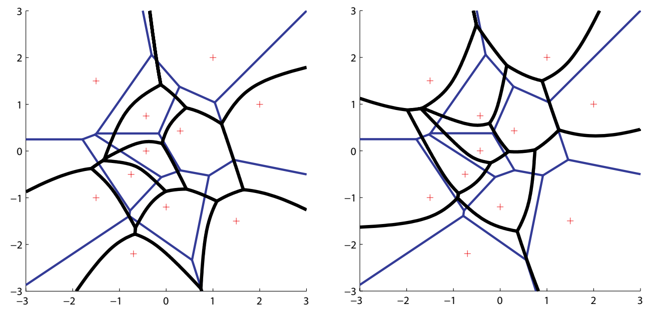

(a) The ZVD (left) and DZVD (right) for the wind field w_1.

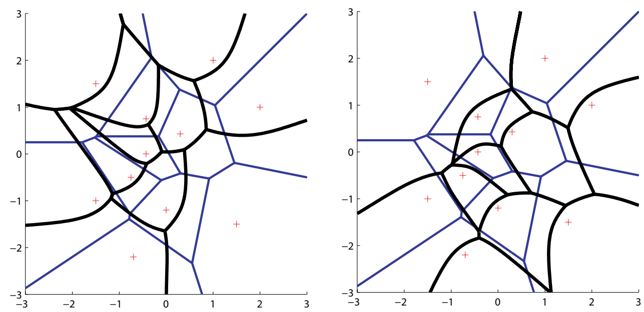

(b) The ZVD (left) and DZVD (right) for the wind field w_2.

Fig. 6. The Zermelo-Voronoi Diagram for two different time–varying wind velocity fields.

References

[1] G. Albers, L. J. Guibas, J. S. B. Mitchell, and T. Roos. Voronoi diagrams of moving points. *International Journal of Computational Geometry and Applications*, 8(3):365 – 380, 1998.

[2] F. Aurenhammer. Voronoi diagrams: A survey of a fundamental geometric data structure. *ACM Computing Surveys*, 23(3):345 – 405, 1991.

[3] E. Bakolas and P. Tsiotras. Minimum-time paths for a light aircraft in the presence of regionally-varying strong winds. In *AIAA Infotech at Aerospace*, Atlanta, GA, April 20–22 2010. AIAA Paper 2010-3380.

[4] R. G. Bartle. *The Elements of Real Analysis.* Wiley Sons Inc., New York, second edition, 1976.

[5] J-D. Boissonnat. Geometric structures for three-dimensional shape representation. *ACM Transactions on Graphics*, 3(4):266 – 286, 1984.

[6] J-D. Boissonnat and M. Yvinec. *Algorithmic Geometry.* Cambridge University Press, Cambridge, United Kingdom, 1998.

[7] C. Caratheodory. *Calculus of Variations and Partial Differential Equations of First Order.* American Mathematical Society, Washington DC, third edition, 1999.

[8] M. Cesari. *Optimization - Theory and Applications. Problems with Ordinary Differential Equations.* Springer-Verlag, New York, 1983.

[9] J. Cortes and F. Bullo. Coordination and geometric optimization via distributed dynamical systems. *SIAM Journal of Optimization and Control*, 44:1543 – 1574, 2005.

[10] J. Cortes, S. Martinez, T. Karatas, and F. Bullo. Coverage control for mobile sensing networks. *IEEE Transactions on Robotics and Automation*, 20:243 – 255, 2004.

[11] O. Devillers, M. Golin, K. Kedem, and S. Schirra. Queries on Voronoi diagrams of moving points. *Computational Geometry*, 6(5):315 – 327, 1996.

[12] G. L. Dirichlet. Über die Reduktion der Positiven Quadratischen Formen mit drei Unbestimmten Ganzen Zahlen. *Journal für die Reine und Angewandte Mathematik*, 40:209 – 227, 1850.

[13] S. Fortune. A sweepline algorithm for Voronoi diagrams. *Algorithmica*, 2:153 – 174, 1987.

[14] J. Gallier. *Geometric Methods and Applications: for Computer Science and Engineering*. Springer-Verlag, New York, USA, 2000.

[15] H. J. Kelley. Guidance theory and extremal fields. *IRE Transactions on Automatic Control*, AC-7:75 – 82, October 1962.

[16] J. C. Latombe. *Robot Motion Planning*. Kluwer Academic Publishers, Boston, MA, 1991.

[17] S. M. Lavalle. *Planning Algorithms*. Cambridge University Press, New York, NY, 2006.

[18] T. Nishida and K. Sugihara. Voronoi diagram in the flow field. *Lecture Notes in Computer Science*, 2906/2003:26 – 35, 2004.

[19] T. Nishida, K. Sugihara, and M. Kimura. Stable marker-particle method for the Voronoi diagram in a flow field. *Journal of Computational and Applied Mathematics*, 202(2):377 – 391, 2007.

[20] A. Okabe, B. Boots, K. Sugihara, and S. N. Chiu. *Spatial Tessellations: Concepts and Applications of Voronoi Diagrams*. John Wiley and Sons Ltd, West Sussex, England, second edition, 2000.

[21] F. Savla, K. Bullo and E. Frazzoli. The coverage problem for loitering Dubins vehicles. In *Proceedings of of 46th IEEE Conference on Decision and Control*, pages 1398–1403, New Orleans, LA, December 2007.

[22] J. A. Sethian. *Level Set Methods and Fast Marching Methods*. Cambridge University Press, Cambridge, second edition, 1999.

[23] K. Sugihara. Voronoi diagrams in a river. *International Journal of Computational Geometry and Applications*, 2:29 – 48, 1992.

[24] G. F. Voronoi. Nouveles applications des paramètres continus à la théorie de formas quadratiques. *Journal für die Reine und Angewandte Mathematik*, 134:198 – 287, 1908.

[25] E. Zermelo. Über das Navigationproble bei Ruhender oder Veranderlicher Windverteilung. *Z. Angrew. Math. und. Mech.*, (11), 1931.